.

The hydrophilic and hydrophobic effects on the structure and themodynamic properties of confined water: water in solutions

Francesco Mallamace,[1,2] Domenico Mallamace,[3] Sow-Hsin Chen,[1] Paola Lanzafame,[4] and Georgia Papanikolaou[4]

[1)] *Department of Nuclear Science and Engineering, Massachusetts Institute of Technology, Cambridge, MA 02139, USA*

[2)] *Istituto dei Sistemi Complessi, Consiglio Nazionale delle Ricerche, 00185 Roma, Italy*[a)]

[3)] *Departments of ChiBioFarAm and MIFT - Section of Industrial Chemistry, University of Messina, CASPE-INSTM, V.le F. Stagno d'Alcontres 31, Messina, 98166, Italy*

[4)] *Departments of ChiBioFarAm - Section of Industrial Chemistry, University of Messina, CASPE-INSTM, V.le F. Stagno d'Alcontres 31, Messina, 98166, Italy*

(Dated: 5 March 2021)

NMR Spectroscopy is used, in the temperature range 180-350K, to study local order and transport in liquid water (pure and confined) and its solutions with glicerol and methanol at different molar fractions. Being the liquid water thermodynamic dominated by polymorphism (two coexisting liquid phases: high- and low-density HDL and LDL) - with the LDL due to the hydrophilic HB interactions, originating in the supercooled regime the tetrahedral networking and the liquid-liquid transition - we focused our interest to hydrophobic effects (HE) on these. Nowadays, if compared to the hydrophilicity, little is known about hydrophobicity so that the main purpose of this study is to gain new information on it. We measured the relaxation times (T_1 and T_2) and the self-diffusion (D_S). From the times we took advantage of the NMR property to follow the behaviors of each molecular component (the hydrophilic and hydrophobic groups) separately; they are studied directly and D_S in terms of the Adam-Gibbs model: obtaining the configurational entropy (S_{conf}) and the specific heat contributions ($C_{P,conf}$). Due to the HE all the studied quantities, behave differently. For water-glycerol the HB interaction is dominant for all the conditions, whereas for water-methanol are observable two different T-regions above and below 265 K, dominated respectively by the hydrophilicity and hydrophobicity. A situation linked to the water polymorphism. Below this temperature, where the LDL phase and the HB networking develops and grows, the times and $C_{P,conf}$ change behaviors leading to maxima and minima. Above it, where the HB becomes weak and less stable and the HDL dominates, the hydrophobicity determines the solution properties.

Keywords: water, local order, relaxation times, self-diffusion, hydrophobic effect.

[a)]Electronic mail: (francesco.mallamace@unime.it)

I. INTRODUCTION

Water represents one of the most interesting research material; the reasons for this are in the central role in many research fields as far as for its unusual thermodynamics, if compared with normal liquids[1]. It is well known to researchers that almost all of its properties have an anomalous behavior as a function of thermodynamic variables, especially in the metastable supercooled liquid regime below its melting temperature T_m up to the homogeneous nucleation temperature (T_h)[2]. The best known of these is the maximum in its density (ρ) at $277K$, whereas, very important to understand the system chemical-physics are also the pressure (P) and temperature (T) behaviors of the thermodynamic response functions. In particular, the isobaric specific heat (C_P), the compressibility (isothermal κ_T and adiabatic κ_S) and the expansivity (α_P); all describing the local fluctuations in volume (δV) or entropy (δS).

These fluctuations in a regular liquid are positively correlated and decrease as T decreases, whereas for water, below T_m, they not only grow but become anticorrelated (an increase in V brings an entropy decrease). Thus, supercooled water is governed by a growing development in its local order so that, as observed by Speedy and Angell[3], the mentioned response functions have diverging (critical like) behaviors. For ambient pressure the diverging temperature is $T_S \sim 228K$.

Another characteristic of the water in the solid crystalline phase is the polymorphism, i.e. the ice has many different structural forms ranging from the ice Ic to ice XII[4]. After the Mishima discovery of the "polyamorphism"[5,6], i.e. the existence of glassy forms with different densities, the idea of a liquid polymorphism[7–11] has been confirmed. Specifically, Mishima discovered the water high-density amorphous phase (HDA), whereas the low-density amorphous phase (LDA) obtained, at low T, by the pressure-amorphization of the ice (I_h) was known since 1935[12]. These two amorphous phases can be transformed into each other respectively through a reversible first order transition[13]. Furthermore, at ambient pressure, LDA if heated undergoes a glass to liquid transition (at about $130K$) into a highly viscous fluid and then crystallizes at $T_x = 150K$. Another amorphous water, the VHDA (very high density amorphous), was recently discovered[14].

The water knowledges have received a marked improvement after the discovering of its liquid polymorphism: i.e. the high- and low-density liquids, HDL and LDL. The LDL has an

"open" structure governed by a networking process with a tetrahedral symmetry due to the noncovalent attractive hydrogen bonding (HB) interaction. Under precise thermodynamic conditions HDL and LDL can coexists and by changing pressure or temperature they can change one into the other by means of a first order transition: the liquid-liquid transition hypothesis (LLT). An original idea, this last due to a MD study, that taking into account the discontinuity of the LDA-HDA transition, has become central in the water studies being at the base of the liquid-liquid critical hypothesis (LLCP or second critical point in distinction to the vapor-liquid one)[15].

In contrast to the HB there are in water also an intermolecular Coulomb repulsion between electron lone-pairs on adjacent oxygen atoms and two H-O covalent bonds originated by the sharing of the electron lone pairs. Hence, the HB dominates water in the stable and supercooled regime, the repulsive lone pairs mainly influence the water physics from above the boiling temperature (T_b) in the sub-critical and critical region. The vapor-liquid critical point CP is located at: $T_C = 647.1K$, $P_C = 22.064MPa$ and the LLCP it is estimated, by MD experiments, to be located near 200 K and at a pressure less than $200.064MPa$.

The entropy decrease, the diverging behavior observed in water response functions, as well as its liquid polymorphism can explain its anomalies and complexity; through them the presence of a water molecular tetrahedral local order has been experimentally demonstrated. Unfortunately, in spite of the very large number of accurate computational studies, with their positive and proper suggestions[16], the corresponding criticality (inside the supercooled regime) is far to be experimentally proven. Today it seems to be a fascinating chimera for experimental physics, although we are sure of the liquid polymorphism and in particular of the LDL phase favored by the temperature decrease and the corresponding growth of the hydrophilic interaction represented by the hydrogen bond. As proposed by many simulation studies and experimental data (also developed in confined water) the LDL tetrahedral symmetry is that of ordinary ice, in which each water molecule has four nearest neighbors and acts as a H-donor to two of them and a H-acceptor for the other two. A T decrease involves both a growth in sizes of structural networking and its greater stability: the HB lifetime strongly increases (many orders of magnitude) from picoseconds values characteristic of the stable liquid water[17]. However, it must be stressed, that whereas the ice tetrahedral network is permanent, the liquid water tetrahedrality instead is local and transient. It should be noted that a pressure increase contrasts these ordering effects.

The bulk liquid water in principle cannot exist stably in the region between the homogeneous nucleation temperature (T_h) and that in which the ultra-viscous liquid obtained from the fusion of LDA crystallizes (T_x). However, if water is confined in nano-pores smaller than the nucleation centers this constraint can be overcome and water can be easily maintained in the liquid state also in the range $T_h - T_x$ and the LDA can be also achieved[18]. Other ways to explore these low temperature regions is to study water in solutions, or inside ice, or on the outside, as water of hydration, of macromolecules (many of biological interest) and micellar systems[19], or by melting a multimolecular thickness of an ice surface[20]. In such a way many important water properties due to the polymorphism were discovered, like e.g. the existence of a density minimum[21,22], as predicted more than a century ago by Percy W. Bridgman[23] and subsequently confirmed by computational studies[24–28]. Other important results concern the dynamics of the system such as the crossover from a fragile to a strong glass-forming material, originally predicted by Angell[29] and observable at ambient pressure at $T_L \simeq 225$ K[30]; this is also in the water $P - T$ phase diagram, the locus of the Stokes-Einstein relation violation (due to the onset of the dynamical heterogeneities and the decoupling between the translational and rotational modes) and of the Widom line. This last line strongly linked to the LLCP (hence to the LDL and HDL) identifies the maximum in the δV and δS fluctuations where thermodynamic response functions reach their extremes (minimum with negative values in the α_P and maxima in C_P and κ_T).

As known, confined water is involved in a very large part of material systems, in particular in those of biological interest[31]. In these situations, the hydrogen bond (and the system polymorphism) plays an important role although the hydrophobic interaction is equally fundamental. Hydrophobicity is shown in aqueous solution by the nonpolar substances aggregation which excludes water and therefore moieties with these properties characterize amphiphilic molecules. Both these interactions are of fundamental importance in many fields of science and technology. A relevant example is the role played by both in the folding-unfolding of proteins. Unfortunately, in opposite to the well described hydrophilicity, little is known about hydrophobicity. Amphiphiles are usually organic compounds with a head (polar if ionic or HB if non-ionic) and an apolar aliphatic chain (hydrophobic groups), that contact with water molecules which strongly avoid each other[32].

The amphiphile properties, are just defined by these two opposite conditions; in water or oil solutions the single molecule cannot satisfy both, while a cluster of molecules can,

and building blocks of mesoscopic structures are formed under stable thermodynamical conditions[33]. Many polymers and polyelectrolytes containing both a water-insoluble (or oil-soluble) component with a water-soluble component belong to this class of materials. This is the "soft condensed matter" made of complex mesoscopic materials (like long helical rods (e.g., polypeptides, DNA, RNA, and proteins), discoid organic molecules, polymers, colloids, and many different multimolecular-associated structures (membranes and bilayers)) that, despite their complexity, can be described in terms of current statistical physics by means of scaling laws and the concept of universality[34,35].

Past studies, many theoretical and computational (see e.g. ref.s[36–38]) addressed the solutes effect on the solvent (structure and energetics[39]), but despite of the many attempts we don't have yet any analytical forms for quantitatively treat hydrophobicity. An experimental measurement of the pair distribution function between hydrophobic molecules lacks, as well as the corresponding potential of mean force between the two of these molecules. Hence, we are unable to understand the forces underlying hydrophobic interactions and to evaluate their implications[40]. New experiments are thus necessary in order to give the bases for a quantitative theory of hydrophobic effects that enables the study of complex materials including bio-systems. However, just by using water confined in hydrophobic nanotubes, it has been experimentally demonstrated (by means of nuclear magnetic resonance (NMR)) that the hydrophobicity becomes effective only in the high T regime ($T > 281K$)[41].

There are many solutes with chemical moieties that affect the water HB ordering process, e.g., the ion charges in salt solutions or the hydrophobic heads in simple alcohols and polymer systems. At the same time the macromolecular functions (peptides, proteins, and DNA) are affected by their interaction with water and in particular by the hydrophilic/hydrophobic contrast, meaning that water is not simply a solvent but an integral and active component. It is itself a sort of "biomolecule" that plays both a dynamic and structural role[42]. Summarizing, water interactions, hydrophilic and hydrophobic, are thus key elements in determining its properties and functions in all the material science, including biological materials where water is essentially in a confined state.

Recent NMR studies, made at the thermal denaturation of an hydrated protein (lysozyme), have clearly confirmed these suggestions showing that the hydrophilic (the amide NH) and hydrophobic (methyl CH_3 and methine CH) peptide groups evolve and exhibit different temperature behaviors. This clarifies the role of water and hydrogen bonding in the stabilization

of protein configurations[43]. The data have also revealed the role of hydrophobic effects in this important protein intramolecular process and on the water properties. These findings, together with two NMR studies (the aforementioned confined water in carbon nanotubes[41] and a recent on water-methanol solutions[44]), have suggested the present work, that shows a detailed study of water properties in two different solutions: glycerol and methanol at many different water molecular fraction X_W and in a very large temperature range ($180 - 350$ K), including the stable and the supercooled region where the polymorphism is relevant in determining the water properties.

In this frame we have considered the differences in the sizes of these amphiphiles, in their boiling points (glycerol 563 K and methanol 337.8 K) and their overall thermal behavior: i) the glycerol melting temperature is $T_M = 291$ K so that for the large part of the studied T water is confined in a supercooled liquid, viceversa having the methanol its $T_M = 175.3$ K water is always in solution within a liquid; ii) the glycerol has an a high molecular weight, if compared to that of water, ($M_{WG} = 92.112$, and $M_{WW} = 18,015$ g/mol) and iii) a molecular structure ($C_3H_5(OH)_3$ made of three hydrophilic hydroxylic groups (OH), two external and one central, besides a central CH and the two external methylenes (CH_2)-hydrophobic). The methanol ($M_{WM} = 32.04$) is more simple (CH_3OH), a methyl group linked to a hydroxyl group). Between the two solutes, methanol, due to the methyl group, is certainly of high and effective hydrophilicity if compared to that of the glycerol.

The study, essentially addressed to verify, at different temperatures and concentrations, the water behavior "confined" in these two liquids and the resulting effects of the hydrophobic-hydrophilic molecular competition, is developed by considering the available water transport functions (self-diffusion and relaxation times) as well as the measured specific heats of the three pure liquids. In addition, form the self-diffusion we will evaluate, in the frame of the Adam-Gibbs approach (developed for glass-forming supercooled liquids to clarify their cooperative relaxation processes[45]), both the configurational entropy S_{conf} and the corresponding $C_{P,conf}$. Some important aspects of the molecular hydrophobic effect will be clarified from the behaviors of the measured NMR spin-spin (T_2) and spin-lattice (T_1) relaxation times.

II. DATA AND DATA ANALYSIS

Figure 1 illustrates the self-diffusion data, D_S, of pure water, glycerol and methanol and their water solutions (many come from NMR and the other from the dielectric experiments and measured as relaxation times (DE). Many data have been measured by us just for this work (specifically for the water-methanol solutions (**Figure 1A**) at $X_W = 0.95, 0.9, 0.8, 0.7, 0.6, 0.5, 0.4$ for $T < 278$ K ; in the water-glycerol case (**Figure 1B**) the measured concentrations are $X_W = 0.9, 0.8, 0.7, 0.6, 0.5, 0.4$ for $T < 290$ K). All the other data come from literature: for the methanol solutions ref.s[46–53] and for those of the glycerol ref.s[46,54–58]. For water, reported data, are coming from different experimental approaches: bulk water data (reported as fully blue symbols) come from NMR experiments[59,60], fused amorphous water (dark blue squares[20]) and MCM confined (NMR actual data are proposed as dark blue squares and previous open blue triangles[30], finally the dielectric relaxation data[61] are illustrated as blue open circles).

We carried out NMR experiments using a Bruker AVANCE NMR spectrometer operating at a 700MHz ^{1}H resonance frequency, and we measured the D_S using the pulsed gradient stimulated echo technique (^{1}H-PGSTE) and the sample temperature stability was maintained in the range $\pm$0.2K. The inversion recovery pulse sequence was used to measure the spin-lattice relaxation T_1, varying the inter-pulse delay from microseconds to several seconds, and the spin-spin relaxation (T_2) was obtained from the Carr-Purcell-Meiboom-Gill procedure. The samples are prepared at the desired water molar fraction using pure glycerol and methanol (99.9%, from Fisher Scientific) and double distilled water.

From the proposed D_S data, **Figure 2**, are evident two different behaviors from the methanol and glycerol solution at the different T. Whereas in the glycerol case (right panel) the behavior is regular and continuous for all the concentrations (a T change affects only the slope), for the methanol solutions (left panel) at the highest temperatures, in the range $1 > X_W > 0.5$, a decrease in the water content corresponds to a D_S decrease with a minimum at $X_W \simeq 0.5$. Always for methanol solutions, below a certain temperature on going in the water supercooled regime, the D_S data change curvature from concave to convex. These behaviors in the local dynamical data (like the self-diffusion or the mean-square displacement) can be due to the hydrophobic effect, present in both solutions, but with different results due to the different molecular sizes of the three substances, their thermodynamical status (stable

liquid or supercooled) and on the number of their hydrophilic (OH) and hydrophobic (CH, CH_2 and CH_3) groups. Considering all this, their comparable molecular weights and the equivalent probability between a HB or a hydrophobic repulsion the water and methanol molecular dynamics will be certainly very sensitive to the hydrophobic effect, when these substances are in solution. The opposite is true for glycerol-water solutions where three water molecules are in principle necessary to saturate with HBs the three OH groups of a single glycerol molecule. In any case, these effects should be opposed by the HB water networking (and the LDL development and growth) by supercooling.

III. RESULTS AND DISCUSSIONS

A. NMR relaxation time data.

This situation is well clarified from the temperature and concentration evolution of the measured T_2 and T_1 NMR relaxation times, reported in **Figure 3** and **4**. The first one reports these times measured in the range $335 > T > 200$ K for all three pure materials, where differences between the values of the different substances and different thermal evolutions are observable. It can be observed for both water and glycerol that in some temperature ranges the two times assume identical values: for water for $T < T_m$ whereas for glycerol this happens at higher temperatures. In the past glycerol, being (like water) a sort of prototype of a glass-forming material, it has been characterized through different experimental techniques, in particular NMR[62,63]. The main question was whether or not its molecular units C_3H_5 and O_3H_3 had the same time behavior, or would behave differently when approaching the dynamic arrest. More specifically a combination of ^{2}H-NMR spin-lattice relaxation and quasi-elastic neutron scattering experiments (that measure the total mean square displacement ($\langle r^2 \rangle$) - equivalent in a Brownian approximation to D_S ($\langle r^2 \rangle = 2D_S t$) on deuterated glycerol ($C_3H_5(OD)_3$ and $C_3D_5(OH)_3$) revealed that the corresponding measured T_1 have the same temperature behavior except beyond the glass transition (whereas the absolute values differ for a factor of ~ 1.6)[63]. In particular, if normalized to the coupling constant of the bonds C-^{2}H and O-^{2}H they assume identical values for $T < T_g$, indicating that the ^{2}H spins of these bonds are subjected to the same motion. This study also stress that amplitudes and activation energies of C-bonded and O-bonded hydrogens are different, with the

O-H motion of larger translational amplitude and higher activation energy. These results evidence that the dynamics in a water-glycerol solution will be essentially dominated by the glycerol molecules with a linear behavior as that proposed in **Figure 2**. **Figure 3**, instead, explain the different behaviors on the NMR relaxation times of the three materials. Those corresponding to water (are reported only bulk water data) and methanol have values that decrease as T decreases and ranges, with comparable values, from $0.1 - 10$ sec. In the glycerol case these times vary from 10^{-6} to 0.1 and the spin-lattice relaxation time has a minimum (~ 0.8 ms at about 280 K, after than increases). For the water-glycerol solutions NMR experiments (T_1 and T_2) made in the region $283 - 383$ K have fully confirmed the same linearity of behavior, as a function, of the composition and temperature shown by the transport parameters[64,65]. It has been also shown, that these solutions are essentially dominated by the HB interaction: the presence of water increases the overall glycerol mobility and glycerol slows down the mobility of water[66].

Being thus interested to the hydrophobic effect we considered to measure the NMR relaxation times in the methanol water solutions, also taking into account these comparable differences in the corresponding times of the pure liquids, considering the fact that some of them cross at a certain T, so we have caried out their measurements in the mixture of the two substances even at the different molar fractions of water. The corresponding data, for $X_W = 0.95, 0.9, 0.8, 0.6, 0.5$ and 0.3 are reported in **Figure 4**, which illustrates the obtained results on reporting in the top panel T_2, whereas the spin-spin relaxation times are in the bottom one. As it can be observed, both for pure water and for the lower concentrations of methanol, the data are limited (compared to the others X_W) and stop at the lowest temperatures at the solidification point of the sample. The observable results in both figures are surprising and interesting as they propose some behaviors typical of bulk water as well as clarify some properties of the hydrophobic effect. Starting from T_1, bottom of the **Figure**, the solution data, in all the contributions (OH_W, OH_M and CH_3) show a well-defined minimum at the temperature of the dynamical strong-fragile crossover of the water, i.e. $T_L \simeq 225$ K, where the phase LDL and the HB networking[30,67] are dominant. Furthermore, the values and the behavior of the spin-lattice relaxation times of the two hydroxylic groups are identical, although smaller than those measured in bulk water, while those of the methyl groups are slightly larger.

However, as reported in the top of **Figure 4**, the behaviors measured in the corresponding

spin-spin relaxation times are more intriguing. What is immediately noticed is that the solution values are essentially lower than those of the pure components and that at the temperatures of the stable liquid water the values corresponding to the methyl group are higher (two orders of magnitude) than those of the two hydroxyl groups, but at the lowest T their behavior is identical with a maximum, just at $T_L \simeq 225$, where all the measured spin-lattice times have a minimum. More precisely, at high temperatures (while T decreases) the values corresponding at the two hydroxyls show a well-defined minimum located within the experimental error at ~ 315 K. This temperature is for water a remarkable thermodynamic property: it is the place of the minimum, at all pressures, of isothermal compressibility ($\kappa_T(P,T)$) and also represents the point where all the lines of the expansivity ($\alpha_P(P,T)$) cross each other[68]. It has also been suggested that it is the locus of the onset of the HB tetrahedral structure[69,70].

On decreasing T, the T_2 dynamics are completely uncorrelated up to about 265 K (where the methyl spin-spin times have a minimum), after than on approaching the deep supercooled regime methyl and hydroxyls times assume identical thermal behavior. This is a significant result, in other words the reported data show that this latter temperature (265 K) represent a crossover for the hydrophobic effect: below it, the solution dynamics is dominating by the hydrophilicity (HB interaction) but above it the hydrophobicity and its effects are certainly active and relevant.

B. Configurational effects.

After these results, to better clarify the observed effects, we took into consideration the hypothesis of treating the self-diffusion data of both solutions (as well as of the three substances) with the Adam-Gibbs model calculating the configurational contributes to their entropies and specific heats. In this context, the $C_P(T)$ values measured (**Figure 5a**) in the three substances both in the liquid phase (stable and supercooled) and in the solid phase are proposed as a function of the temperature. **Figure 5a** together with the specific heats of glycerol[71], water[72–74] and methanol[75] also shows (vertical dotted lines) their melting temperatures. It can be therefore observed that for glycerol and water many values belong to the metastable state of supercooled liquid. The figure also shows that the specific heats of water and methanol cross at about 265 K. While below this temperature, those of water

are greater than those of methanol, for higher values it is the methanol that has higher and increasing values. As theoretically proposed for water we can assume[76] that the difference between the liquid and solid specific heat can give a good estimation of the configurational contribution, such a difference for the three substances, $C_{P,conf} \simeq \Delta C_P = C_{P,liq} - C_{P,sol}$, as evidenced in the **Figure 5b.**

The well-known Adam-Gibbs model (AG) is a molecular-kinetic theory, which explains the relaxation temperature dependence of glass-forming liquids. It was explained in terms of the T-variation in the size of the cooperatively rearranging regions. In particular, it is shown that these sizes are determined by configuration restrictions, which can be expressed in terms of their configurational entropy. According to this the transition probability $W(T) = Fexp(-z\Delta\mu/k_BT)$ of a cooperative region is evaluated as a function of its size z and $\Delta\mu$ (the potential energy hindering cooperative rearrangements), where F is a frequency factor (negligibly $T-$dependent) and k_B the Boltzmann constant. By expressing the "critical size" z^* of the cooperative region in terms of the molar configurational entropy S_{conf} the transition probability can be expressed as $W(T) = Aexp(-C/TS_{conf})$. Being the system relaxation times related to the transition probability as: $\tau(T) \propto W(T)^{-1}$, we have

$$D_S(T) = D_{S0} \exp(-A/TS_{conf}) \tag{1}$$

D_{S0} and $A = z\Delta\mu$ can be assumed as constant (at a given concentration). By using such an approach the water configurational $C_{P,conf}$ was evaluated from the bulk water diffusion data (measured and simulated in the range 373 - 237 K)[76] obtaining $D_{S0} = 1.07\ 10^{-7}$ m^2sec^{-1} and $A = 31.75$ $kJmol^{-1}$. Very recently the same analysis was made by considering the self-diffusion data of confined water using satisfactorily the same values of D_{S0} and A[77].

A and S_{conf} can be thus evaluated by using Eq. 1 in the bulk systems as far as in all the considered water solutions whereas a proper value of D_{S0} was estimated from the $D_S(T)$ in the high T limit. Having in such a way obtained S_{conf} the final step of the work was the $C_{P,conf}$ calculation as $C_{P,conf} = T(\partial S_{conf}/\partial T)_P$. Such a derivative was made after a fit of the entropy data by means of a a sixth-order polynomial in temperature. **Figure 6** reports, as a function of T, the configurational entropy S_{conf} (top) and $C_{P,conf}$ (bottom) for water, glycerol and methanol. For the water cases we report also the contributions coming from confined (and fused) water measured well inside the supercooled region up to the amorphous phases[20,30,61]. The obtained values of D_{S0W} and A_W are the same as those of the original

simulation study which gave for the first time the evidence of a maximum in C_P due to the water polymorphism (maximum experimentally observed in confined water[78] and here confirmed by using the AG). For glycerol and methanol $D_{S0G} = 4.3\ 10^{-7}$ and $D_{S0M} = 6.7\ 10^{-7}\mathrm{m^2sec^{-1}}$, and $A_G = 23.1$ $A_M = 51.15$ $\mathrm{kJmol^{-1}}$ are respectively obtained.

After these results, also the solutions configurational entropies have been evaluated and the corresponding results are shown in the **Figure 7** (at the top there are the water-methanol data and that of water-glycerol are at the bottom). As it can be observed in the methanol solutions, the S_{conf} behavior at higher T ($T > 260$ K) is not continuous: the value of pure water entropy is higher than that of the solutions in the X_W range $0.9 - 0.4$. This S_{conf} behavior is, as proposed by the NMR findings on the spin-spin relaxation time, due to a local order, not related to the HB networking, but driven by the hydrophobic effect.

The entropy excess observed on mixing water with hydrophobic species, and the consequent non-ideal changes in other thermodynamical quantities, was defined by Kauzmann[79] as the challenging problems in the physics of aqueous solutions. This after the pioneering work of Frank and Evans[80] who proposed the idea that the hydrophobic entities enhance the water structure towards a more ordered one near to the alcohol head groups. Lately, the alcohol-water correlations were studied using MD simulation[36–40,81] and experimentally[55,56,82–84], by confirming this local enhanced order. This indicate, that nowadays, there is consensus that hydrophobic entities affect the water structure. The water pair correlation functions are sharpened, if compared to those of the pure liquid, with the consequent possibility of a hydration sphere around hydrophobic entities. Finally, from the reported S_{conf}, by performing the corresponding derivatives, for all the studied pure materials and solutions, the configurational specific heats $C_{P,conf}$ have been evaluated (**Figure 8a)**. The Figure also illustrates and compares the corresponding ΔC_P as that observed for the $C_{P,conf}$ coming from pure glycerol, methanol and water. In all the three cases the data obtained can be superimposed with the corresponding experimental values after a multiplication for a constant factor C_W, C_{Me} and C_{Gly}, but as can be seen their T dependence is the same of the ΔC_P. An equal procedure is necessary for the different water concentrations, but in this case the used multiplicative factor is evaluated, according to the molar fraction, as $C = X_W C_W + (1 - X_W) C_{Me}$ (or C_{Gly}) and the obtained data are shown in the **Figure 8a** (the error bar is the same of the symbols size). A significant result is that for both solutions a $C_{P,conf}$ maximum can be observed for samples in which we have $0.5 < X_W < 1$, indicating that the HB networking and water

polymorphism dominates the resulting structure for both solutions to the lowest T. Another observation comes from the data evolution of the methanol solution at the temperatures of the stable liquid water phase: the resulting $C_{P,conf}$ temperature evolution is analogous to that of methanol rather than of water, thus indicating, in accordance with NMR data, some effect of methanol on the water caging.

This latter situation becomes clearer if we look at the total specific heat of the water-methanol system reported in **Figure 8b**; the corresponding C_P are obtained by adding at the $C_{P,conf}$ the X_W weighted values of the two solid phases. What these data show finally, clarifies that in this high temperature region the behavior of the solutions is dominated by the methanol. In fact, from the overall behavior of the reported data a crossover temperature is evident ($\sim$ 265 K) above which the methanol specific heat and those of the different solutions are higher than that of pure water, while in the opposite case the specific heats for water and those of the solutions dominate on the corresponding methanol data.

IV. CONCLUSION

Starting from the current research findings that water is also in the liquid phase dominated by a polymorphism generated by the HB interactions and that this polymorphism, made from the LDL and HDL phases, as proposed by the LLT model[15], dominates the behavior of thermodynamical functions, also clarifying the origin of the anomalies that characterize the system, we evaluated the idea to study effects or interactions contrary to the formation of HB networking and therefore to the LDL phase. In this context, also in order to adequately analyze the system in the supercooled regime, where the LDL is dominating, we have considered confined water. But unlike water in nanotubes we have thought of solutions, in which water remains liquid even at low temperatures; solutions with non-polar substances which, instead, possess both hydrophilic and hydrophobic groups: i.e. with a head that supports or promotes the HB interaction (and the corresponding networking) and a tail that is unfavorable to it, therefore hydrophobic.

In such a way it was therefore possible to study on a molecular scale their contrasting effects on the structure and physical-chemical properties of both the solvent and the solute. In this context we have chosen glycerol and methanol. The former is together with water a prototype of a supercooled glass-forming liquid with a comparative large molecular weight

and a different internal structure made of three hydrophilic groups and as many hydrophobic tails. Methanol, instead has a molecular weight comparable to that of water (and a similar mobility) with a hydrophilic and a hydrophobic head so that it can act alternatively either as HB supporter or as its destroyer. With this approach, considering the water confined in the respective solutions (water-glycerol and water-methanol) and using an experimental technique, such as NMR, sensitive to both order and dynamics on a molecular scale, it was be possible to clarify some aspects of the hydrophobic effect (which represents the central point of this study).

We evidenced the temperature evolutions of the spin-spin (T_2) and the spin-lattice (T_1) relaxation times as far as the self-diffusion coefficient (D_S) in the range $180 - 350$K. In the first case we took advantage of the NMR property to follow the behaviors of each molecular component separately (at the same time), so that we have measured distinctly all the hydrophilic and hydrophobic groups of the different molecules (water, glycerol, methanol and of their solutions). On the contrary the self-diffusion data, according to the used ^{1}H-PGSTE method deal with the motion of the entire molecule. The data obtained for these three transport functions were then compared with those reported in the literature.

While the relaxation time behaviors are analyzed directly, the data related to self-diffusion have been studied according to the Adam-Gibbs model. In this latter case, the aim was to highlight the behavior of the configurational entropy and the corresponding specific heat contribution.

Operating in this way, the main result obtained from all the studied quantities, with regard to the "confined" water in the two solutions, appears to be different in relation to the two interactions of interest (hydrophilic and hydrophobic). While in the first case (water-glycerol) the HB interaction appears dominant for all the studied temperatures and concentrations, in the second case (water-methanol) the presence of two different temperature regions, dominated separately by the hydrophilicity and hydrophobicity, is evident. The crossover temperature between these regions is located at ~ 265 K. Such a situation also appears to be linked to the polymorphism of water and to the relative balance between the LDL and HDL phases. In fact, below this crossover temperature, where the LDL phase (and therefore the HB networking) develops and grows, the NMR relaxation times and configurational specific heat show extremes (maximum and minimum) just at the temperature of the supercooled liquid water dynamical crossover and of the Widom line (**Figures 4**, **6**

and **8**). Instead above this temperature (265 K), where the HB becomes weak and less stable and therefore dominates the HDL phase, the hydrophobic effect determines the solution properties.

In conclusion, the main message of the present study is that, like the HB, the hydrophobic effect is strongly T-dependent, but it affects the aqueous solutions properties in opposite temperature regions. This latter is a situation of great importance regarding the properties of many macromolecular systems, where water is confined. Such a competition between the basic interactions of the system can determine in them, by changing the thermodynamic variables, significant configurational evolutions.

AUTHOR'S CONTRIBUTIONS

All authors contributed equally.

V. ACKNOWLEDGEMENT

The MD work was supported by the European Project H2020 A-LEAF - 732840; LP and GP benefited from the national PRIN 2017 project (Italy).

VI. DATA AVAILABILITY

The data that support the findings of this study are available from the corresponding author upon reasonable request..

REFERENCES

[1]P. Ball, Life's Matrix: A Biography of Water, 1st ed.; Farrar, Straus, and Giroux: New York, 2000; pp xvi, 417.

[2]P. G. Debenedetti and H.E. Stanley, H. E. *Phys. Today* **56**, 40-46 (2003).

[3]R.J. Speedy and C.A. Angell, *J. Chem. Phys.* **65**, 851-858 (1976).

[4]C. Lobban, J. L. Finney e W. F. Kuhs, *Nature* **391**, 268–270 (1998).

[5]O. Mishima, L.D. Calvert and E. Whalley, *Nature* **310**, 393-397 (1984); ibd. *Nature* **314**, 76-78 (1985).

[6]O. Mishima, *Nature* **384**, 546-550 (1996).

[7]E. Rapoport, *J. Chem. Phys.* **46**, 2891 (1967).

[8]G. Nemethy and H. Scheraga, *J. Chem. Phys.* **36**, 3382 (1962).

[9]C. M. Davis and T. A. Litovitz, *J. Chem. Phys.* **42**, 2563 (1965)

[10]M. S. Jhon, J. Grosh, T. Ree, and H. Eyring, *J. Chem. Phys.* **44**, 1465 (1966).

[11]B. Kamb, *Science* **150**, 205 (1966).

[12]E. F. Burton and W.F. Oliver, *Proc. R. Soc. London, Ser. A*, **153**, 166-172 (1935).

[13]O. Mishima, *J. Chem. Phys.* **100**, 5910-12 (1994).

[14]T. Loerting, C. Salzmannm, I. kohl, E. Mayer and A. Hallbrucker, *Phys. Chem. Chem. Phys.* **3**, 5355 (2001).

[15]P.H. Poole, F. Sciortino, U. Essmann and H.E. Stanley, *Nature*, **360**, 324-328 (1992).

[16]J.C. Palmer, P.H. Poole, F. Sciortino and P.G. Debenedetti, *Chem. Rev.* **118**, 9129-9151 (2018).

[17]F. X. Prielmeier, E. W. Lang, R. J. Speedy, and H.-D. Lüdemann, *Ber. Bunsenges, Phys. Chem.* **92**, 1111-1117 (1988).

[18]S. Cerveny, F. Mallamace, J. Swenson, M. Vogel and L. M. Xu, L. M. *Chem. Rev.* **116**, 7608-7625 (2016).

[19]F. Mallamace, P. Baglioni, C. Corsaro, J. Spooren, H. E. Stanley, and S.-H. Chen, *Riv. Nuovo Cimento* **34**, 253 (2011).

[20]Y. Xu, N. G. Petrik, R. Scott Smith, B. D. Kay, and Greg A. Kimmel, *Proc. Natl. Acad. Sci. USA* **113**, 14921–14925 (2016).

[21]F. Mallamace, C. Branca, M. Broccio, C. Corsaro, C.-Y. Mou, and S.-H. Chen, *Proc. Natl. Acad. Sci. USA* **104**, 18387–18391 (2007).

[22]M. Erko, D. Wallacher, A. Hoell, T. Hauß, I. Zizak, and O. Paris *Phys. Chem. Chem. Phys.* **14**, 3852–3858 (2012).

[23]P.W. Bridgman, *Proc. Am. Acad. Art. Sci.* **47**, 441–558 (1912).

[24]J. L. Abascal and C. Vega, *J. Chem. Phys.* **133**, 234502 (2010).

[25]J. L. Abascal and C. Vega, *J. Chem. Phys.* **134**, 186101 (2011).

[26]Y. Ni and J. L. Skinner, *J. Chem. Phys.* **144**, 214501 (2016).

[27]J. A. Sellberg et al., *Nature* **510**, 381–384 (2014).

[28]K. H. Kim, A. Späh, H. Pathak, F. Perakis, D. Mariedahl, K. Amann-Winkel, J. A. Sellberg, J. H. Lee, S. Kim, J. Park, K. H. Nam, T. Katayama, and A. Nilsson, *Science*

358, 1589–1593 (2017).

[29]K. Ito, C. T. Moynihan and C. A. Angell, Nature **398**, 492 (1999).

[30]S. H. Chen, F. Mallamace, C. Y. Mou, M. Broccio, C. Corsaro, A. Faraone and L. Liu, Proc. *Natl. Acad. Sci. USA*, **103**, 12974-12978 (2006).

[31]H. E. Stanley, S. V. Buldyrev, G. Franzese, P. Kumar, F. Mallamace, M. G. Mazza, K. Stokely and L. Xu, J. Phys.: Condens. Matter **22**, 284101 (2010).

[32]S. A. Safran, Statistical thermodynamics of surfaces, interfaces and membranes. (Addisonr-Wesley, Reading, 1994).

[33]P. G. de Gennes and J. Prost, The physics of liquid crystals. (Oxford Science Publication, Oxford, 1974).

[34]P. Flory, Principles of polymer chemistry. (Cornell University Press, Ithaca, 1953).

[35]P. G. de Gennes, Scaling concepts in polymer physics. (Cornell University Press, Ithaca, 1979).

[36]H. S. Ashbaugh and L. R. Pratt, *Rev. Mod. Phys.*, 78, 160-178 (2006).

[37]P. Ball, *Chem. Rev.*, **108**, 74-108 (2008).

[38]Y. E. Altabet and P. G. Debenedetti, *J. Chem. Phys.* **147**, 241102 (2017).

[39]B. Widom and D. Ben-Amotz, *Proc. Natl. Acad. Sci.* USA **103**:18887 (2006).

[40]D. Chandler, *Nature* **437**, 640–647 (2005).

[41]H.J. Wang, K.K. Xi, A. Kleinhammes and Y. Wu, *Science* **322**, 80–83 (2008).

[42]Y. Levy and J.N. Onuchic, *Ann. Rev. Biophys. Biomol. Struct.* **35** 389–415 (2006).

[43]F. Mallamace, C. Corsaro, D. Mallamace, S. Vasi, C. Vasi, P. Baglioni, S.V. Buldyrev, S.H. Chen and H.E. Stanley, *Proc. Natl. Acad. Sci. USA* **105**, 536 (2016).

[44]D. Mallamace, S.H. Chen, C. Corsaro, E. Fazio, F. Mallamace and H.E. Stanley, *Sci. China-Phys. Mech. Astron*, **62**, 107003 (2019).

[45]G. Adam and J. H. Gibbs, *J. Chem. Phys.* **43**, 139 (1965).

[46]C. Corsaro, R. Maisano, D. Mallamace, and G. Dugo, *Physica A* **392**, 596–601 (2013).

[47]N. Karger, T. Vardag, and H.-D. Ludemann, *J. Chem. Phys.* **93**, 3437 (1990).

[48]D. J. Denney and R.H. Cole, *J. Chem. Phys.* **25**, 1767 (1955).

[49]H. Mandal, D. G. Frood, M. A. Saleh, Bi. K. Morgan, and S. Walker, *Chem. Phys.* **134**, 441–451 (1989).

[50]B.P. Jordan, R.J. Sheppardt, and S Szwarnowski, *J. Phys. D: Appl. Phys.* **11**, 695 (1978).

[51]D. Bertolini, M. Cassettari, and G. Salvetti, *J. Chem. Phys.* **78**, 365 (1983).

[52]G. A. Noyel, L. J. Jorat, O. Derriche, and J. R. Huck, *IEEE Trans. on Elect.Ins.* **27**, 113 (1992).

[53]M. Sun, L-M. Wang, Y. Tian, R. Liu, K. L. Ngai, and C. Tan, *J. Phys. Chem. B* **115**, 8242–8248 (2011).

[54]A. Puzenko, Y. Hayashi, Y. E. Ryabov, I. Balin,Y. Feldman, U. Kaatze, and R. Behrends, *J. Phys. Chem. B*, **109**, 6031-6035 (2005).

[55]B. Chen, E. E. Sigmund, and W. P. Halperin, *Phys. Rev. Lett.* **96**, 145502 (2006).

[56]I. Popov, A. Greenbaum, A. P. Sokolov and Y. Feldman, *Phys. Chem. Chem. Phys.* **17**, 18063 (2015).

[57]K. Schröter, and E.J. Donth, *Chem. Phys.* **113**, 9101 (2000).

[58]J. Trejo Gonzalez, M. P. Longinotti, and H. R. Corti, *J. Chem. Eng. Data* **56**, 1397 (2011).

[59]J. H. Simpson and H. Y. Carr, *Phys. Rev.* **111**, 1201 (1958).

[60]W.S. Price, H. Ide, and Y. Arata, *J. Phys. Chem. A* **103**, 448-450 (1999).

[61]J, Sjöström, J. Swenson,R. Bergman and S. Kittaka, *J. Chem. Phys.* **128**, 154503 (2008).

[62]M. Wolfe and J. Jonas, *J. Chem. Phys.* **71**, 3252 (1979).

[63]F. Fujara, W. Petry, R. M. Diehl, W. Schnauss and H. Sillescu, *Europhys. Lett.* **14**, 563 (1991).

[64]N. Bloembergen, E. M. Purcell and R. V. Pound, Phys. Rev., **73** 679 (1948).

[65]V. Aroulmoji and A.S. Rao, *Phys. Chem. of Liquid*, **38**, 723 (2000).

[66]A. V. Egorov, A. P. Lyubartsev and A. Laaksonen, *J. Phys. Chem. B*, **115**, 14572–14581 (2011).

[67]F. Mallamace, M. Broccio, C. Corsaro, A. Faraone, D. Majolino, V. Venuti, L. Liu, C.Y. Mou and S.H. Chen, *Proc. Natl. Acad. Sci. USA* **104**, 424-428 (2008).

[68]F. Mallamace, C. Corsaro and H.E. Stanley, *Sci. Rep.* **2**, 993 (2012).

[69]F. Mallamace, C. Corsaro, D. Mallamace, C. Vasi, and H. E. Stanley, *Farad. Disc.* **167**, 95 (2013).

[70]J. Catalán and J. C. del Valle, *ACS Omega* **3**, 18930-18934 (2018).

[71]G.E. Gibson and W.F. Giauque, *J. Am. Chem. Soc.*, **45**, 93 (1923).

[72]D.G. Archer and R.W. Carter, *J. Phys. Chem. B*, **104**, 8563 (2000).

[73]E. Tombari, C. Ferrari and G. Salvetti, *Chem. Phys. Lett.*, **300**, 749 (1999).

[74]Y.P. Handa, O Mishima and E. Whalley, *J. Chem. Phys.*, **84**, 2766 (1986).

[75]K.K. Kelley, *J. Am. Chem. Soc.*, **51**, 180 (1929).

[76]F. Starr, C.A. Angell and H.E. Stanley, *Physica A*, **323**, 51 (2003).

[77]F. Mallamace, C. Corsaro, D. Mallamace, E. Fazio, S.H. Chen and A. Cupane, Int. J. Mol. Sci. **21**, 622 (2020).

[78]M. Oguni, S. Maruyama, K. Wakabayashi, and A. Nagoe, *Chemistry – An Asian Journal* **2**, 514 (2007); M. Oguni,Y. Kanke and S. Namba, *AIP Conf. Proceed.* **982**, 34 (2008).

[79]W. Kauzmann, *Adv. Prot. Chem.* **14**, 1 (1953).

[80]H. S. Frank and M. J. Evans, *J. Chem. Phys.* **13**, 507 (1945).

[81]N. T. Skipper, *Chem. Phys. Lett.* **207**, 424 (1993).

[82]A. K. Soper and J. L. Finney, *Phys. Rev. Lett.* **71**, 4346 (1993).

[83]N. Micali, S. Trusso, C. Vasi, D. Blaudez and F. Mallamace, *Phys. Rev. E*, **54** 1720 (1996).

[84]F. Mallamace, C. Corsaro, D. Mallamace, C. Vasi, S. Vasi and H. E. Stanley, *J. Chem. Phys.* **144**, 064506 (2016).

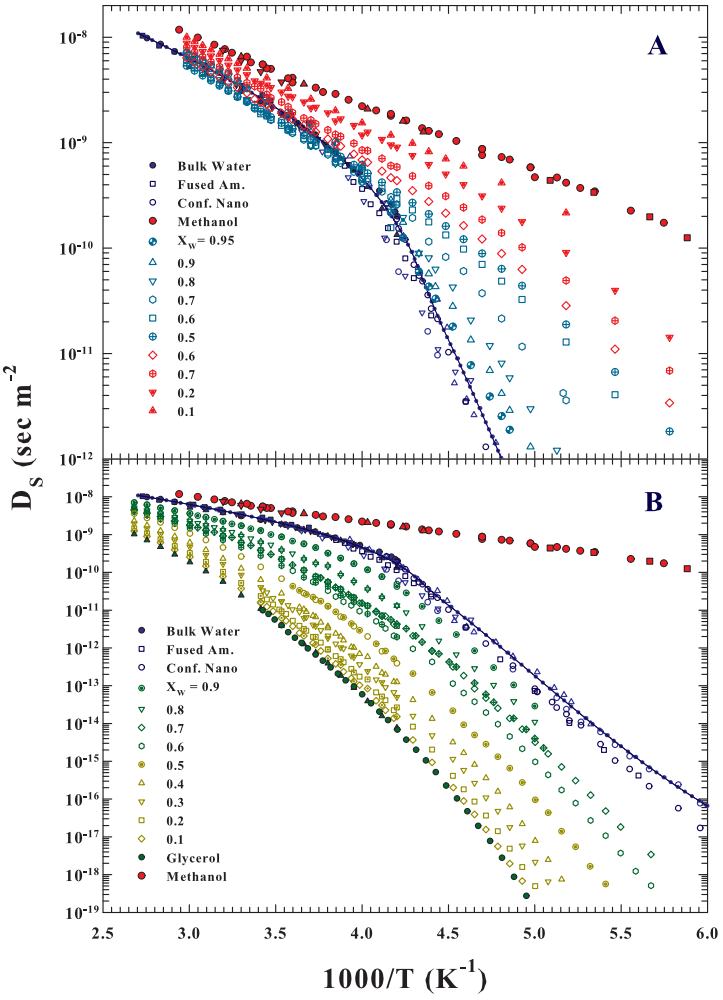

FIG. 1. The self-diffusion, D_S, of pure water, glycerol and methanol and their water solutions (many are measured by using NMR and the other from the dielectric experiments DE). The data are reported in one Arrhenius representation: log D_S vs $1000/T$. Many data have been measured just for this work (specifically for the water-methanol solutions (**Figure 1A**)) at $X_W = 0.95, 0.9, 0.8, 0.7, 0.6, 0.5, 0.4$ for $T < 278$ K. In the water-glycerol case (**Figure 1B**) the measured concentrations are $X_W = 0.9, 0.8, 0.7, 0.6, 0.5, 0.4$ for $T < 290$ K). All the other data comes from the literature: for the methanol solutions ref.s[46–53] and for the glycerol ref.s[46,54–58]. For water are proposed NMR data: i) bulk water data (reported as fully blue symbols[59,60]); ii) fused amorphous water (dark blue squares[20]); iii) MCM confined (actual data are proposed as dark blue squares and previous as blue triangles[30]; iv) finally the dielectric relaxation data[61] (are illustrated as blue open circles). Full and empty symbols represent pure materials and solutions respectively, as far as the different colors.

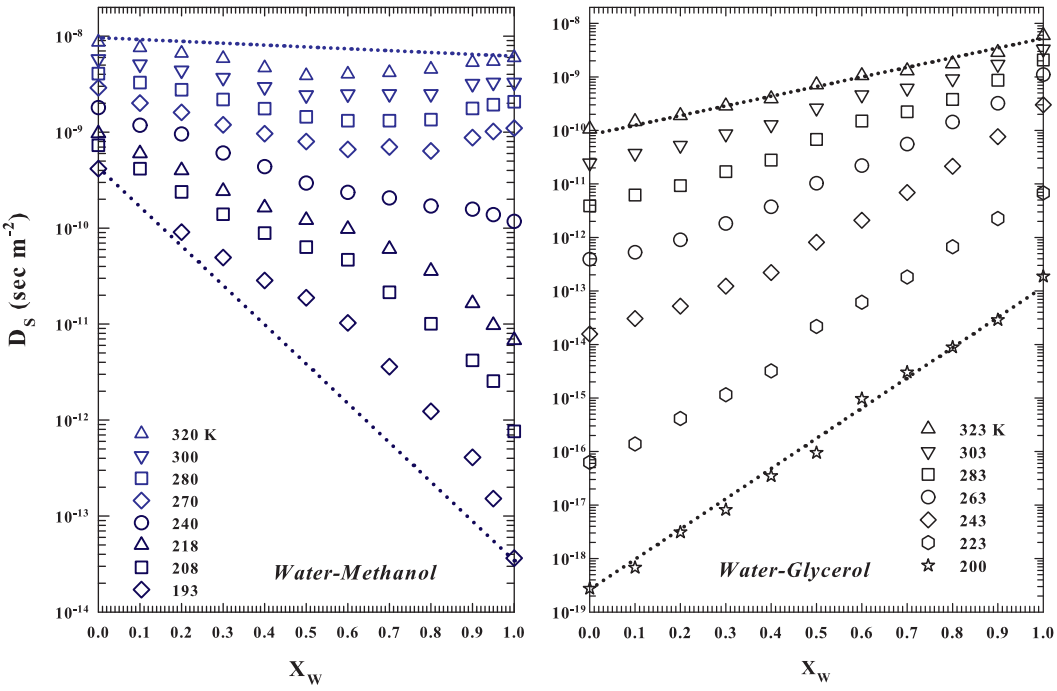

FIG. 2. The two different behaviors in the D_S for the methanol and glycerol solution, as a function of the water molar fraction. at the different$T$. For glycerol solutions (right panel) the behavior is regular and continuous for all the concentration (a T change affects only the slope). Instead, for the methanol solutions (left panel) at the highest T, a decrease in the water content corresponds, range $1 > X_W > 0.5$, to a D_S decrease with a minimum at $X_W \simeq 0.5$. Again, for these latter solutions, below a certain temperature on going in the water supercooled regime, the D_S data change curvature from concave to convex.

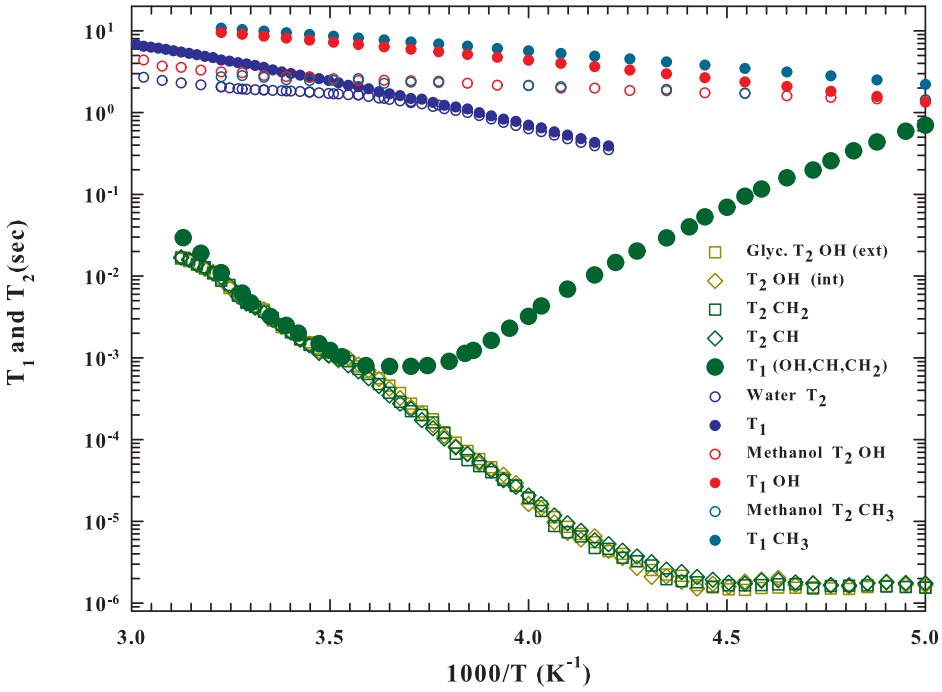

FIG. 3. The Arrhenius representation of the measured spin-spin T_2 and and spin lattice T_1 relaxation times for water, methanol and glycerol. For methanol and glycerol also the behavior of all their different hydrophilic (OH) and hydrophobic (methine CH, methylenes CH_2 and methyl CH_3) are reported.

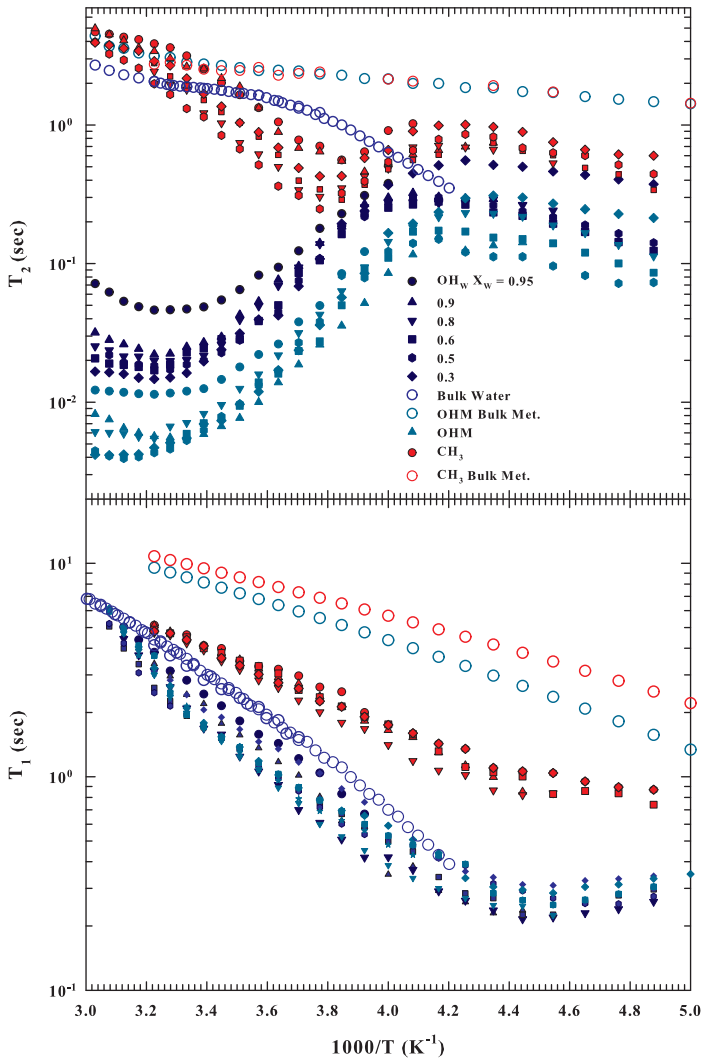

FIG. 4. The Arrhenius representation of the NMR relaxation times T_2 (top) and T_1 (bottom), for water, methanol and their solutions at the following water molar fractions: $X_W = 0.95, 0.9, 0.8, 0.6, 0.5$ and 0.3. Here are reported the measured values of the hydrophilic (OH) groups of water and methanol and methanol hydrophobic group (CH_3), showing well different behaviors.

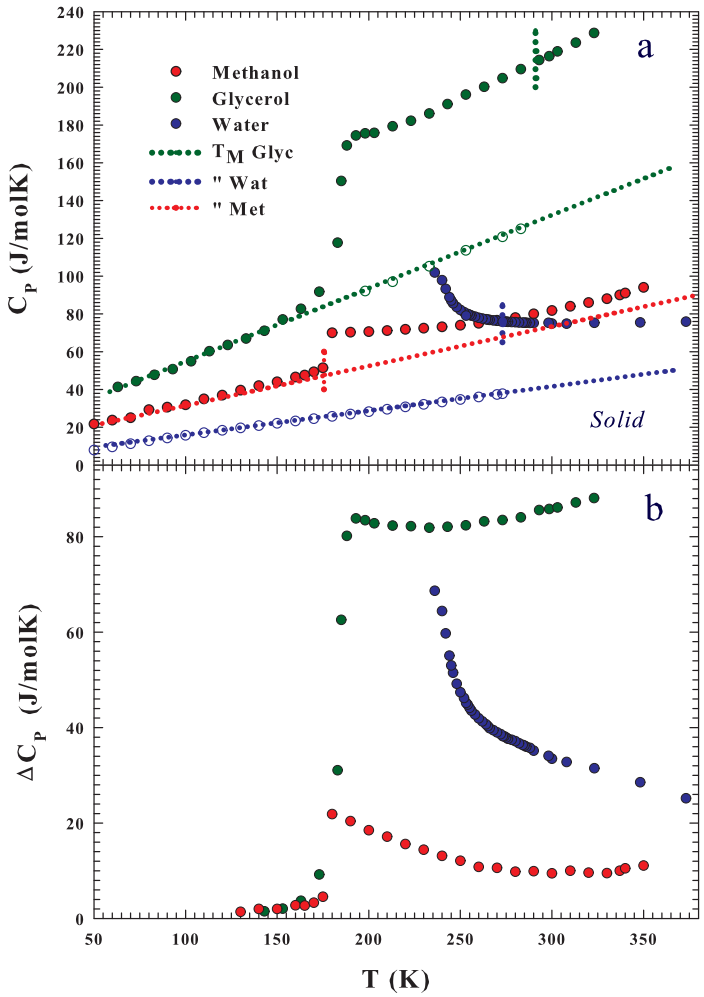

FIG. 5. The water[72–74], methanol[75] and glycerol[71] $C_P(T)$ values, measured (**Figure 5a,** top side) as a function of the temperature, in their liquid (stable and supercooled) and solid phases (straight dotted lines). Their melting temperatures (vertical dotted lines) are also reported. As it can be observed the water and methanol specific heats cross at about 265 K. As theoretically proposed for water we can assume[76] that the difference between the liquid and solid specific heat can give a good estimation of the configurational contribution; such a difference for the three substances, $C_{P,conf} \simeq \Delta C_P = C_{P,liq} - C_{P,sol}$, is proposed in **Figure 5b** (bottom side)**.**

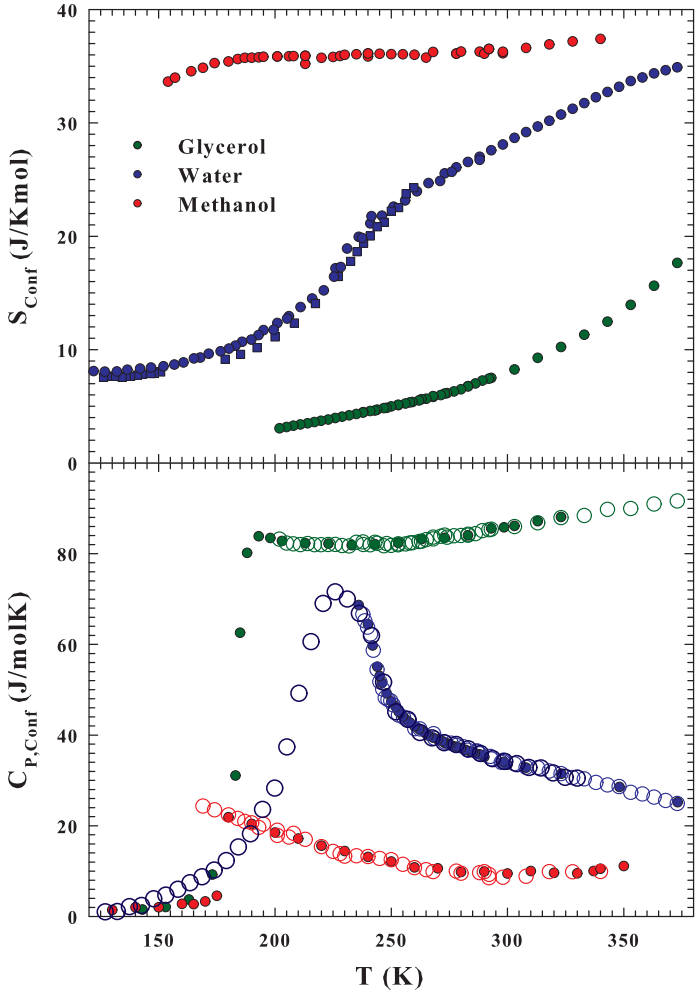

FIG. 6. The water configurational entropies S_{conf} (top side) and the corresponding specific heat contributions $C_{P,conf}$ (bottom) for water, glycerol and methanol, obtained in terms of the Adam-Gibbs model are reported as a function of the temperature. In the water cases are also reported the contributions coming from confined (and fused) water which allowed a measurement of the transport functions well inside the supercooled region up to the amorphous phases[20,30,61].

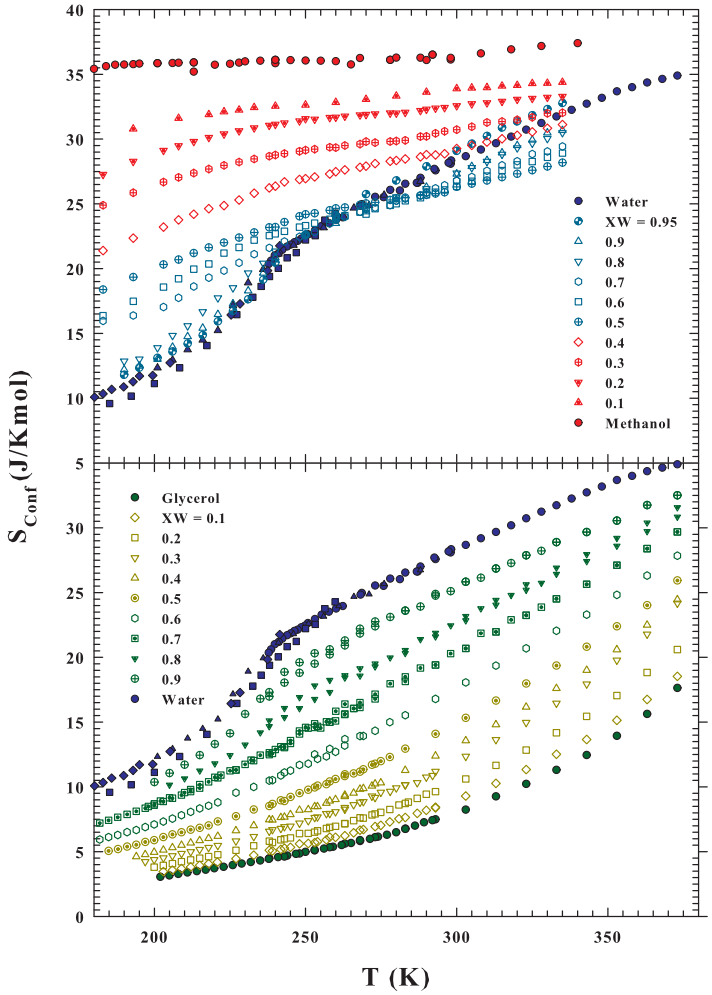

FIG. 7. The solutions configurational entropies evaluated, according with the Adam-Gibbs, are proposed as a function of the temperature. At the top there are the water-methanol data and that of water-glycerol are in the bottom. As it can be observed in the methanol solutions, their behavior at higher T ($T > 260$ K) is not continuous with Xw: the pure water S_{conf} is higher than that of solutions for the X_W range $0.9 - 0.4$. As explained, it is due to the hydrophobic effect as proposed by the NMR findings.

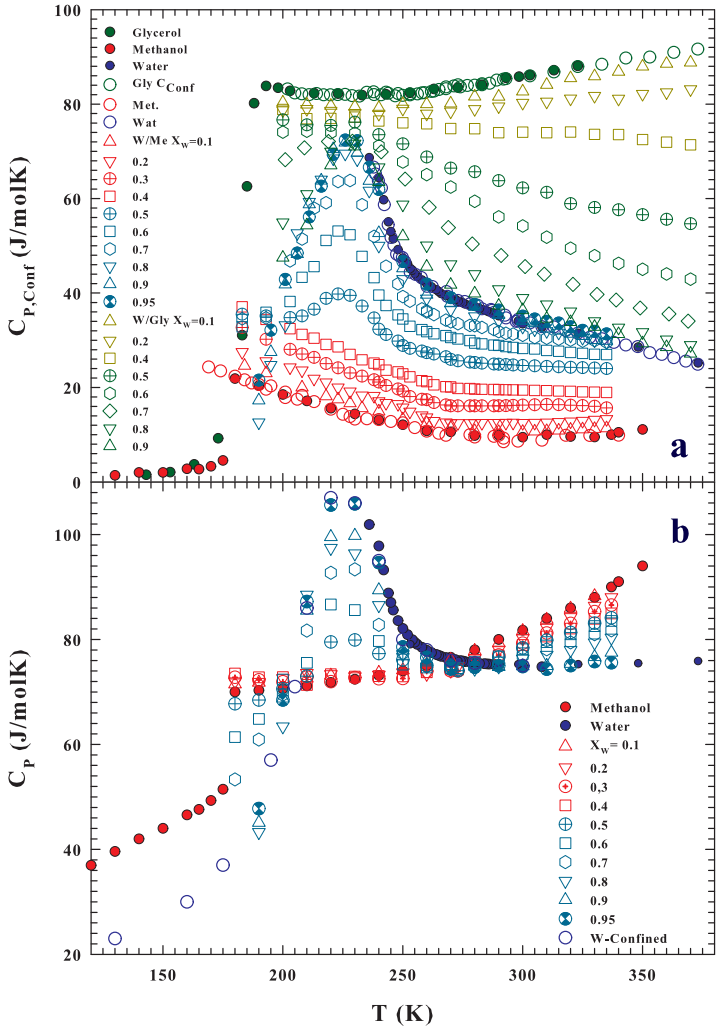

FIG. 8. The configurational specific $C_{P,conf}$ (**Figure 8a,** top side) evaluated, according the Adam-Gibbs, for the different water solutions at their different water molar fractions are illustrated. Are also proposed both the ΔC_P the $C_{P,conf}$ coming from pure glycerol, methanol and water. The bottom side (**Figure 8b**), instead, show total specific heat of the water-methanol system including their solutions data.